

ChemComm

Accepted Manuscript



This is an *Accepted Manuscript*, which has been through the Royal Society of Chemistry peer review process and has been accepted for publication.

Accepted Manuscripts are published online shortly after acceptance, before technical editing, formatting and proof reading. Using this free service, authors can make their results available to the community, in citable form, before we publish the edited article. We will replace this *Accepted Manuscript* with the edited and formatted *Advance Article* as soon as it is available.

You can find more information about *Accepted Manuscripts* in the [Information for Authors](#).

Please note that technical editing may introduce minor changes to the text and/or graphics, which may alter content. The journal's standard [Terms & Conditions](#) and the [Ethical guidelines](#) still apply. In no event shall the Royal Society of Chemistry be held responsible for any errors or omissions in this *Accepted Manuscript* or any consequences arising from the use of any information it contains.

COMMUNICATION

Alkali Metal Oxides Trapped by Diethylzinc

Cite this: DOI: 10.1039/x0xx00000x

L. Zane Miller,^a Michael Shatruk^a and D. Tyler McQuade^{*a}

Received 00th January 2012,

Accepted 00th January 2012

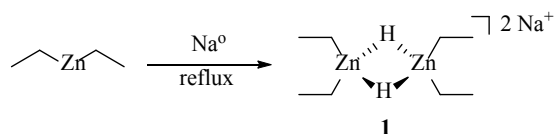
DOI: 10.1039/x0xx00000x

www.rsc.org/

Reactions of alkali metal hydroxides with neat diethyl zinc lead to the formation of oxo-centered clusters $M_2O(ZnEt_2)_n$ ($M = Na, n = 3$ or $M = K, Rb, n = 4$). These molecules crystallize in highly symmetric space groups, forming extended structures supported by weak M-H interactions. We discuss the mechanistic implications and relationship of these structures to known (oxo)organozincates.

The chemistry of diethylzinc, arguably the oldest organometallic compound,¹ is rich and complex.² For example, reactions between diethylzinc and alkali metals have been studied extensively since the key discoveries of Frankland and Wanklyn,³ but the products of such reactions are difficult to characterize and use due to air and moisture sensitivity.⁴ Diethylzinc itself is a volatile pyrophoric liquid that thwarted its crystal structure determination until recently.⁵

These challenges, however, have not impeded the use of dialkylzinc hydride “ate” complexes in organic synthesis because they often exhibit enhanced chemoselective, diastereoselective, and catalytic reductions.⁶ Recently, Lennartson et al. reported the first crystal structure of alkali metal diethylzinc hydride (**1**) formed by reacting sodium metal with neat diethylzinc (Scheme 1).⁷ The structure of this sodium “zincate” contains two intact $ZnEt_2$ molecules bridged by two hydrides with two sodium counter ions. We speculated that the Lennartson zincate might be prepared by refluxing NaH in neat diethylzinc. The outcome of this simple experiment was not as anticipated and opens another chapter in the chemistry of diethylzinc.



Scheme 1 Reaction of sodium metal with excess $ZnEt_2$ to produce **1**.

Refluxing NaH with neat $ZnEt_2$ resulted in dissolution of the hydride followed by crystallization of a product on cooling the solution. Initially, we speculated that the resulting product was the

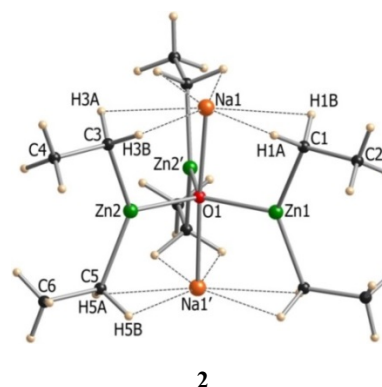


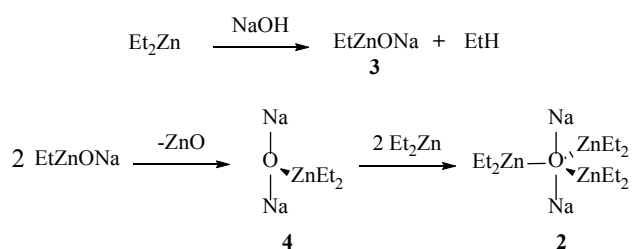
Fig. 1 Molecular structure of $Na_2(ZnEt_2)_3(\mu_5-O)$ (**2**). Selected bond lengths (Å) and angles (°): Zn1-O1: 2.001(3), Zn2-O1: 1.983(1), Zn1-C1: 2.004(4), Zn2-C3: 2.009(3), Zn2-C5: 2.018(3), Na1-O1: 2.278(1), C1-Zn1-C1': 137.0(2), C3-Zn2-C5: 135.8(1), Zn1-O1-Zn2: 121.05(6), Zn2-O1-Zn2': 117.9(1), Zn1-O1-Na1: 88.41(7), Zn2-O1-Na1: 90.26(4), Zn2'-O1-Na1: 91.38(4), Na1-O1-Na1': 176.8(1). ¹H NMR (600 MHz, THF-d₈): δ = 1.12 (t, CH₃), -0.247 (q, CH₂). ¹³C NMR (151 MHz, THF-d₈): δ = 9.64 (CH₃), 0.00 (CH₂).

desired Lennartson zincate, but crystallographic analysis revealed a new $Na_2(ZnEt_2)_3(\mu_5-O)$ (**2**) species. As shown in Figure 1, the compound is comprised of three $ZnEt_2$ units coordinated to a linear sodium oxide fragment, Na_2O .

The presence of the central oxygen atom was surprising, and we originally speculated that molecular oxygen was the source. The reactions of $ZnEt_2$ with water and molecular oxygen are well-known.^{8,9} Importantly, we note that the reactions of O_2 with $ZnEt_2$ inevitably result in insertion of oxygen (or peroxide) into the Zn-C bond.^{8b,8c} In striking contrast, the oxo-centered species shown in Figure 1 does not contain any Zn-O-C bonds. Conversely, water reacts with $ZnEt_2$ to yield $HOZnEt$ that decomposes rapidly at room temperature to zinc oxide and ethane.^{8g} Other reactions involving $ZnEt_2$ and trace water have given rise to products with multiple bound oxygen atoms and cleavage of one of the Zn-Et bonds.^{8h}

Based on these considerations, the lack of Zn-O-C bonded fragments in product **2** would represent quite an unusual scenario if the O atom came from O₂ or H₂O. Therefore, we speculated that the O atom in cluster **2** resulted from the contamination of NaH with sodium hydroxide. Herein, we demonstrate that NaOH, KOH, and RbOH, when reacted with ZnEt₂, produce linear M-O-M fragments surrounded by three or four ZnEt₂ molecules, depending on the radius of the alkali metal ion. In the solid state, these oxo-centered clusters organize via weak M-H bonds to form symmetric and extended structures.

We tested our hypothesis that the oxygen in **2** resulted from NaOH by comparing reactions of ZnEt₂ with pure NaH and Na₂CO₃. When dry NaH or Na₂CO₃ was refluxed with ZnEt₂, product **2** was not observed. The use of NaOH, on the other hand, provided **2** in 22.5% yield after 2 hours of refluxing in neat ZnEt₂. Interestingly, the use of more meticulously dried NaOH produced the same product and byproducts but at a slower rate. Based on these observations and intermediates observed by others,^{8g} we propose the mechanism shown in Scheme 2. Initially, NaOH reacts with ZnEt₂ to form intermediate **3**, which is similar to an intermediate proposed in the hydrolysis of ZnEt₂.^{8g,i} The condensation of **3** into oxo-bridged species **4** is followed by addition of two more ZnEt₂ units to form **2**. This mechanism, however, does not explain the observed reaction rate difference when wet and dry NaOH are used. Unfortunately, the wet NaOH reaction is both violent and undergoes multiple phase changes making rate studies difficult.



Scheme 2 Proposed mechanism for the formation of product **2**.

The structure determination by single-crystal X-ray diffraction[†] revealed that the molecule of **2** contains a nearly linear Na₂O fragment surrounded by three ZnEt₂ units (Figure 1). The two Na⁺ and three Zn²⁺ ions thus form a trigonal-bipyramidal (TBP) oxo-centered cluster. The environment of each Zn²⁺ ion is completed by two ethyl ligands to give a triangular coordination geometry. There are two crystallographically unique Zn centers, with similar Zn-O and Zn-C bond lengths and C-Zn-C angles (Figure 1, caption). The coordination of Na⁺ ions, however, cannot be satisfied by the conventional ligands present in this structure, i.e. the ethyl C atoms and the μ₅-O atom. As a result, the cluster is stabilized by the weak Na-H bonds to the α-hydrogens of ZnEt₂ units. Each Na⁺ ion forms six intramolecular interactions, with five Na-H distances ranging from 2.502 to 2.552 Å and one longer Na-H separation of 2.715 Å. Nevertheless, even the intramolecular coordination to the α-H atoms does not fulfill the needs of the Na⁺ ion, whose unusual coordination environment is completed via additional intermolecular contacts (at 2.407-2.611 Å) to α- and β-H atoms of an ethyl group belonging to the neighboring molecule (Figure 2a) for the total coordination number of ten (one O + nine H atoms).

The bonds between the TBP clusters result in the formation of extended Na-H-bonded columns that pack into a highly symmetric hexagonal structure in a chiral space group *P*6₅22 (the crystal

examined was racemically twinned). Each subsequent TBP is offset from the previous one in order to optimize the Na-H agostic interactions. Due to this offset, each column of TBP clusters propagates in the form of a helix down the *c* axis (Figure 2b), with a repeat unit equal to six clusters. Such structural arrangement results in a very long period of the unit cell along the *c* axis, 43.327(2) Å, while *a* = *b* = 8.7801(5) Å. The seemingly efficient packing of helices in the crystal structure shown in Figure 2c does not involve any significant column-to-column interactions except for van-der-Waals contacts between the peripheral H atoms. Nevertheless, the clusters are packed quite tightly, and the structure does not contain any interstitial solvent molecules (Figure 3). The analysis of crystal packing did not reveal any solvent-accessible voids.

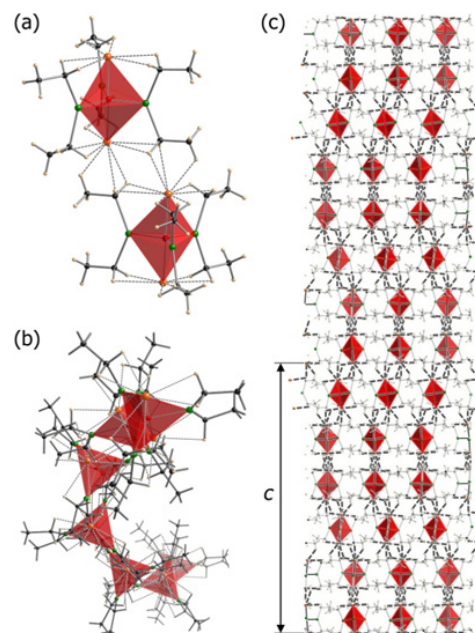


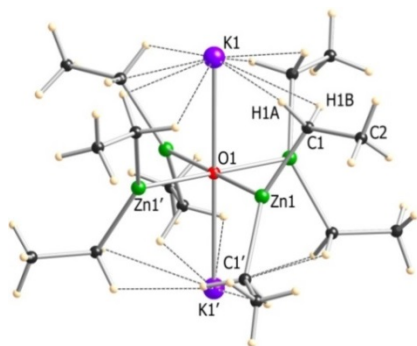
Fig. 2 Crystal packing of **2**: (a) intermolecular interactions between TBP clusters Na₂(ZnEt₂)₃(μ₅-O) that are highlighted with scarlet-red; (b) a helix of Na-H-bonded TBP clusters viewed slightly off the *c* axis; the top and bottom clusters form one repeat unit of the helix; (c) packing of helices viewed perpendicular to the *c* axis. Color scheme: Na = orange, Zn = green, O = red, C = black, H = off-white.

Although agostic interactions are common in organometallic complexes,¹⁰ agostic interactions that dominate and guide crystal packing are less prevalent. We ascribe the formation of the agostically linked framework **2** to the reaction conditions that severely limit the possible coordination modes for the alkali-metal ion. Consequently, the Na-H interactions, while weak, “glue” the clusters together due to the structural necessity. A similar approach was used by Girolami’s group to prepare a molecular complex with one of the highest coordination numbers known for rare-earth metal ions by limiting the metal’s ligation sphere to include only H atoms of aminoboranes.¹¹

The TBP coordination around oxygen is rare in organozinc complexes, with only three examples reported to date.¹² The Zn-O bond distances of 1.983(1) and 2.002(2) Å observed in Na₂(ZnEt₂)₃(μ₅-O) are similar to those reported by Cole et al. for the M₅O core in [(μ₅-O)Li₂Zn₃{(p-tolyl)NC(H)N(O)(p-tolyl)}₆] (1.950-1.990 Å),^{12a} while the Na-O distance of 2.2785(9) Å is naturally longer than the Li-O bonds (1.991 and 1.926 Å) found in the Li₂Zn₃(μ₅-O) cluster.

The unique crystallographic features of **2** prompted us to explore the possibility of reactions between ZnEt_2 and other alkali hydroxides. Hedström *et al.* reported that combination of metallic potassium and ZnEt_2 resulted in a low-yield byproduct, $\alpha\text{-K}_2(\text{ZnEt}_2)_4(\mu_6\text{-O})$.¹³ They speculated that oxygen in the final product originated from adventitious water. Our earlier discussion, however, suggests that the partial hydrolysis of ZnEt_2 cannot lead to such clusters. Therefore, we reacted KOH with neat ZnEt_2 , in analogy to the synthesis of **2**. Once the reaction reached completion, the solid precipitate was filtered off, and the clear colorless solution obtained was layered with dry hexanes. Large colorless crystals were obtained after 24 hours. A single-crystal X-ray diffraction analysis revealed we indeed obtained the desired product, $\beta\text{-K}_2(\text{ZnEt}_2)_4(\mu_6\text{-O})$ (**5**), which crystallized as a different, more symmetric polymorph in comparison to the one reported by Hedström *et al.* The structure of **5** is similar to that of **2**, but the central K_2O fragment is surrounded by four ZnEt_2 units, thus forming an O-centered octahedral cluster of metal ions (Figure 3). The Zn^{2+} ion preserves the triangular coordination environment, but the plane that contains the C–Zn–C bond angle is inclined by 27.1° with respect to the K–O–K axis. A similar distortion is observed in the structure of $\alpha\text{-K}_2(\text{ZnEt}_2)_4(\mu_6\text{-O})$.¹³ The Zn–O and Zn–C bond lengths in **5** (2.816(1) Å) are naturally longer than the Na–O bond in **2** (2.278(1) Å). The larger K^+ ion also requires a larger number of K–H interactions to complete the coordination environment, which explains the presence of four ZnEt_2 units in cluster **5** as compared to three such units in **2**. There are eight intramolecular K–H contacts per K^+ ion that vary from 2.679(1) to 2.779(1) Å. Similar to the structure of **2**, the coordination of the K^+ ion in **5** is completed by four additional intermolecular K–H interactions, resulting in the total coordination number of 13 (one O + twelve H atoms). Noteworthy, however, the intermolecular K–H contacts are significantly longer (3.107 Å) than the intramolecular ones. Nevertheless this structure also does not contain any interstitial solvent molecules or solvent-accessible voids.

In contrast to $\alpha\text{-K}_2(\text{ZnEt}_2)_4(\mu_6\text{-O})$, which crystallizes in the monoclinic space group $C2/c$, the $\beta\text{-K}_2(\text{ZnEt}_2)_4(\mu_6\text{-O})$ polymorph crystallizes in a highly symmetric tetragonal space group $P4/mnc$. The difference stems from the more regular packing of the octahedral $\text{K}_2(\text{ZnEt}_2)_4(\mu_6\text{-O})$ clusters in **5**. In $\alpha\text{-K}_2(\text{ZnEt}_2)_4(\mu_6\text{-O})$, the clusters form K–H bonded layers with the K–O–K axis of the



5

Fig. 3 Molecular structure of $\text{K}_2(\text{ZnEt}_2)_4(\mu_6\text{-O})$ (**5**). Selected bond lengths (Å) and angles ($^\circ$): Zn1–O1: 2.0919(5), Zn1–C1: 2.008(2), K1–O1: 2.817(1), C1–Zn1–C1': 143.8(1), Zn1–C1–C2: 118.2(2), Zn1–O1–Zn1': 90.0, Zn1–O1–K1: 90.0, K1–O1–K1': 180.0. ^1H NMR (600 MHz, THF-d8): δ = 1.18 (t, CH_3), -0.21 (q, CH_2). ^{13}C NMR (151 MHz, THF-d8): δ = 11.97 (CH_3), 3.16 (CH_2).

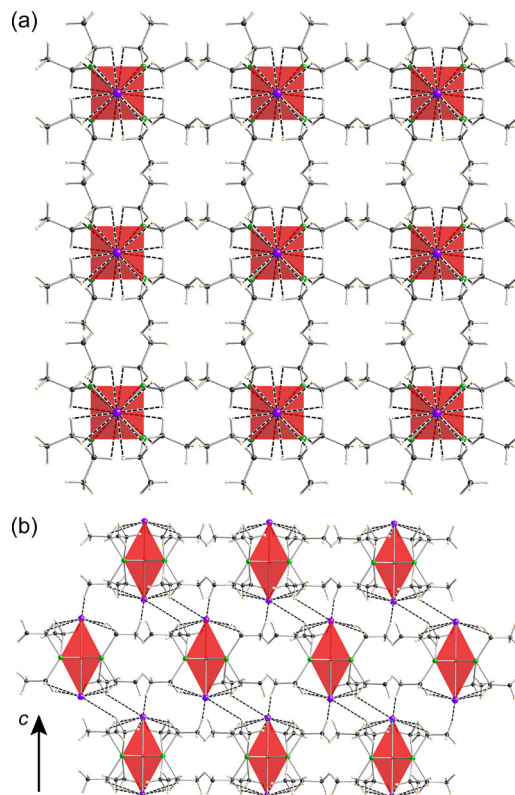


Fig. 4 Crystal packing of **5**: (a) the layer of octahedral clusters $\text{K}_2(\text{ZnEt}_2)_4(\mu_6\text{-O})$ viewed down the c axis (b) the ABAB... stacking of layers along the c axis, with the intermolecular K–H contacts indicated with dashed lines. Color scheme: K = purple, Zn = green, O = red, C = black, H = off-white.

octahedron being parallel to the layer. Consequently, interactions between the layers are restricted to van der Waals contacts between the H atoms of ethyl groups. In $\beta\text{-K}_2(\text{ZnEt}_2)_4(\mu_6\text{-O})$, the octahedral clusters are also packed into layers (Figure 4a), but the K–O–K axis is perpendicular to the layers. As a result, the intermolecular K–H interactions serve to provide interlayer bonding (Figure 4b), while the intermolecular contacts within the layer are due to van der Waals H–H interactions. To optimize the interlayer K–H bonding, the neighbouring layers are shifted with respect to each other, leading to the ABAB... stacking sequence along the c axis (Figure 4b). We believe that the reason for the formation of the more symmetric β -polymorph is the slower controlled crystallization achieved in the present work by the diffusion of hexanes into the ZnEt_2 solution of **5**.

It is interesting to note that in each cluster **5** all C–Zn–C fragments are tilted in the same direction with respect to the K–O–K axis, thus leading to the D_4 molecular symmetry. One layer contains clusters of the same chirality, but the next layer contains clusters of the opposite chirality, thus creating the overall centrosymmetric structure.

Obviously, the size of the alkali-metal ion modifies the coordination requirements and causes the evolution from the TBP cluster **2** to the octahedral cluster **5**. Therefore, one might expect the further increase in the number of the ZnEt_2 units coordinated around the central M_2O fragment if larger alkali-metal ions are used. The reaction between RbOH and ZnEt_2 led to crystallization of $\text{Rb}_2(\text{ZnEt}_2)_4(\mu_6\text{-O})$ (**6**, see SI) that turned out to be isostructural to **5** but showed significantly higher reactivity. The crystals of both **2** and **5** were extremely air- and moisture-sensitive and had to be mounted in an inert-atmosphere dry box. Nevertheless, they could be quickly transferred to the X-ray diffractometer cryostage to collect the

diffraction datasets. In contrast, the crystals of **6** were virtually intolerable to any exposure to air and had to be mounted within a sealed capillary to allow the X-ray data collection. Our attempts to crystallize a similar structure from the reaction of LiOH or CsOH and ZnEt₂ have been unsuccessful thus far, but we are continuing efforts in this direction.

Conclusions

We have demonstrated a simple synthetic route to oxo-centered clusters Na₂(ZnEt₂)₃(μ₅-O) (**2**), K₂(ZnEt₂)₄(μ₆-O) (**5**), and Rb₂(ZnEt₂)₄(μ₆-O) (**6**), which exhibit unprecedented and highly symmetric crystal-packing motifs supported by intercluster interactions between the alkali-metal ions and H atoms of the ethyl groups. These results introduce another aspect of diethylzinc chemistry and an exciting new look at Na₂O which is not typically linear. The reactivity of these species is not understood yet – the compounds definitely react with air and water. How the nucleophilicity of the ethyl ligands or the oxygen atom have changed relative to the non-complexed species is unknown. These data provide general evidence of the aggregation states available to diethylzinc under anhydrous conditions. The observations are similar to complex coordination structures formed by alkyl lithium species.¹⁴ The highly symmetric crystal structures of **2**, **5**, and **6** offer an interesting principle of 3-D structural organization via weak agostic M-H interactions. The effective packing of clusters results in the prolonged stability of these structures in air-free environment, and thus these complexes might serve as solid-state sources of diethylzinc that could show different reactivity patterns as compared to the neat liquid ZnEt₂.

Notes and references

We would like to acknowledge the NSF (awards CHE-1152020 and CHE-0911109) and Chemring, Inc. for support. DoD (DOTC 13-01-INI518) is also acknowledged for support.

^a Department of Chemistry and Biochemistry, Florida State University, 95 Chieftan Way, Tallahassee, Florida 32306, USA. Fax: 850-644-8281; Tel: 850-644-3810; E-mail: mcquade@chem.fsu.edu

†Crystal data for **2**: Zn₃Na₂OC₁₂H₃₀, *M* = 432.45, hexagonal, *P*6₅22, *a* = 8.7801(5), *c* = 43.327(2) Å, *V* = 2892.6(4) Å³, *Z* = 6, λ = 0.71073 Å, 173 K, 18994 reflections collected, 2329 unique (*R*_{int} = 0.025), Flack parameter 0.03(3), GooF = 1.153, *R*₁ = 0.023, *wR*₂ = 0.052 for 105 parameters/0 restraints [*I* > 2σ(*I*)]. CCDC 988444. Crystal data for **5**: Zn₄K₂OC₁₆H₄₀, *M* = 588.16, tetragonal, *P*4/*nnc*, *a* = 9.027(2), *c* = 14.145(3) Å, *V* = 1152.6(5) Å³, *Z* = 2, λ = 0.71073 Å, 173 K, 5225 reflections collected, 697 unique (*R*_{int} = 0.030), GooF = 1.100, *R*₁ = 0.019, *wR*₂ = 0.038 for 30 parameters/0 restraints [*I* > 2σ(*I*)]. CCDC 988445. Crystal data for **6**: *M* = 680.90, tetragonal, *P*4/*nnc*, *a* = 9.446(3), *c* = 14.199(5) Å, *V* = 1266.8(9) Å³, *Z* = 2, λ = 0.71073 Å, 260 K, 7169 reflections collected, 774 unique (*R*_{int} = 0.063), GooF = 1.008, *R*₁ = 0.047, *wR*₂ = 0.106 for 30 parameters/0 restraints [*I* > 2σ(*I*)]. CCDC 988446.

Electronic Supplementary Information (ESI) available: Synthetic and crystallization details; CIF files for compounds **2**, **5**, and **6**. See DOI: 10.1039/c000000x/

- (a) E. Frankland, *Ann.* 1849, **71**, 213; (b) E. Frankland, *Q. J. Chem. Soc.* 1850, **2**, 297.
- D. Seyferth, *Organometallics*, 2001, **20**, 2940.
- (a) J. A. Wanklyn, *Ann.* 1858, **107**, 125; J. A. Wanklyn, *Q. J. Chem. Soc.* 1859, **11**, 103; (b) J. A. Wanklyn, *Ann.* 1858, **108**, 67; (c) J. A. Wanklyn, *Proc. R. Soc. London* 1857-1859, **9**, 341.

- (a) F. W. Frey, Jr., P. Kobetz, G. C. Robinson and T. O. Sustrunk, *J. Org. Chem.* 1961, **26**, 2950; (b) P. Kobetz and W. E. Becker, *Inorg. Chem.* 1963, **2**, 859; (c) G. J. Kubas and D. F. Shriver, *J. Am. Chem. Soc.* 1970, **92**, 1949.
- J. Bacsá, F. Hanke, S. Hindley, R. Odedra, G. R. Darling, A. C. Jones and A. Steiner, *Angew. Chem. Int. Ed.* 2011, **50**, 11685.
- M. Uchiyama, S. Furumoto, M. Saito, Y. Kondo and T. Sakamoto, *J. Am. Chem. Soc.* 1997, **119**, 11425.
- A. Lennartson, M. Håkansson and S. Jagner, *Angew. Chem. Int. Ed.* 2007, **46**, 6678.
- (a) H. W. Thompson and N. S. Kelland, *J. Chem. Soc.* 1933, 756; (b) C. H. Bamford and D. M. Newitt, *J. Chem. Soc.* 1946, 688; (c) S. Jana, R. J. F. Berger, R. Fröhlich, T. Pape and N. W. Mitzel, *Inorg. Chem.* 2007, **46**, 4293; (d) J. Lewiński, W. Marciniak, J. Lipkowski and I. Justyniak, *J. Am. Chem. Soc.* 2003, **125**, 12698; (e) J. Lewiński, K. Suwała, M. Kubisiak, Z. Ochal, I. Justyniak and J. Lipkowski, *Angew. Chem. Int. Ed.* 2008, **47**, 7888; (f) J. M. Grévy in *Encyclopedia of Inorganic Chemistry, 2nd edition* (Eds: R. A. Scott, D. Atwood, C. M. Lukehart, R. H. Crabtree and R. B. King) John Wiley & Sons, New York, 2011; (g) R. J. Herold, S. L. Aggarwal, and V. Neff, *Canadian J. Chem.* 1962, **41**, 1368; (h) A. Pettersen, A. Lennartson, and M. Håkansson, *Organometallics* 2009, **28**, 3567; (i) R. Boomishankar, P.I. Richards, A. Steiner *Angew. Chem. Int. Ed.* 2006; **45**, 4632.
- (a) A. E. H. Wheatley, *Chem. Soc. Rev.* 2001, **30**, 265; (b) D. Prochowicz, K. Sokolowski and J. Lewiński, *Coord. Chem. Rev.* DOI: 10.1016/j.ccr.2013.12.003.
- M. Brookhart, M. L. H. Green, G. Parkin, *Proc. Natl. Acad. Sci. U.S.A.* 2007, **104**, 6908.
- S. R. Daly, P. M. B. Piccoli, A. J. Schultz, T. K. Todorova, L. Gagliardi, G. S. Girolami, *Angew. Chem. Int. Ed.* 2010, **49**, 3379.
- (a) M. L. Cole, D. J. Evans, P. C. Junk and L. M. Louis, *New J. Chem.* 2002, **1**, 1015; (b) C. K. Williams and A. J. P. White, *J. Organomet. Chem.* 2007, **4**, 912; (c) C. Redshaw, S. Jana, C. Shang and M. R. J. Elsegood, *Chem. Commun.* 2010, **46**, 9055.
- A. Hedström and A. Lennartson, *J. Organomet. Chem.* 2011, **696**, 2269.
- J. S. Renny, L.L. Tomasevich, E. H. Tallmadge, D. B. Collum *Angew. Chem., Int. Ed.* 2013, **52**, 2.